Pressure-Driven Chemical Disorder in Glassy As$_2$S$_3$ up to 14.7 GPa, Post-Densification Effects and Applications in Materials Design

Emmanuel Soignard,[1] Oleg B. Tsiok,[2] Andrey S. Tverjanovich,[3] Aleksei Bytchkov,[4] Anton Sokolov,[5] Vadim V. Brazhkin,[2] Chris J. Benmore,[6] and Eugene Bychkov[5,*]

[1] The Eyring Materials Center, Arizona State University, Tempe, Arizona 85287-8301, United States
[2] Institute for High Pressure Physics, Russian Academy of Sciences, Troitsk, Moscow 108840, Russia
[3] Department of Chemistry, St. Petersburg State University, 198504 St. Petersburg, Russia
[4] European Synchrotron Radiation Facility, CS 40220, 38043 Grenoble Cedex 9, France
[5] LPCA, Université du Littoral Côte d'Opale, 59140 Dunkerque, France
[6] Advanced Photon Source, Argonne National Laboratory, Argonne, Illinois 60439, United States

Supporting Information

Computational details of preliminary AIMD modeling.

Figure S1. Glassy As$_2$S$_3$ sample for high-precision compressibility measurements.

Figure S2. Compressibility extrapolation up to 15 GPa using a Murnaghan-type fitting with free V_0.

Figure S3. X-ray structure factors of glassy As$_2$S$_3$ at ambient pressure.

Figure S4. Comparison of the low-Q features in amorphous arsenic, glassy As$_2$S$_3$, and liquid sulfur.

Figure S5. Pressure dependences of the PP1 and PP2 parameters in the $S_X(Q)$ of liquid and glassy As$_2$S$_3$.

Figure S6. X-ray structure factors of liquid and glassy As$_2$S$_3$ at comparable pressure.

Figure S7. FSDP parameters for liquid and glassy As$_2$S$_3$ as a function of pressure.

Figure S8. Total correlation functions $T_X(r)$ for g-As$_2$S$_3$ at ambient pressure and recovered from 11.9 GPa.

Figure S9. Apparent changes of the first neighbor peak at ≈2.28 Å with increasing pressure.

Figure S10. Low-Q diffraction features in glassy As$_2$Te$_3$ and vitreous As$_{0.15}$Te$_{0.85}$.

Figure S11. Crystal structure of monoclinic orpiment As$_2$S$_3$.

Figure S12. Neutron-weighted partial correlation functions $T_{ij}(r)$ in monoclinic As$_2$S$_3$.

Computational details of preliminary AIMD modeling

The Born-Oppenheimer molecular dynamics calculations were performed with the CP2K package (https://www.cp2k.org/) using the generalized gradient approximation and the PBEsol exchange-correlation functional.[S1] Basically, the employed AIMD technique was similar to that used in previously published reports on analogous chalcogenide glass systems.[S2-S4] Randomly generated initial configurations of 1000 atoms (400 As and 600 S) were optimized using RMC++ code[S5] to obtain a good agreement with neutron and high-energy X-ray diffraction results for g-As_2S_3 at ambient pressure. The cubic box size was chosen to match the experimental number density. Further optimization was carried out using DFT with the consecutive basis sets SZV, DZVP and TZVP. The AIMD simulations included sample annealing above the glass transition temperature, 50 ps at 500 K using a Nosé–Hoover thermostat chain controlling the temperature,[S6,S7] and the final modeling over 50 ps at 300 K. A reduction (cold compression) of the simulation box[S8,S9] was then applied to increase the pressure up to 1.3 GPa. The reduced box size was chosen to match the compressibility of g-As_2S_3.

Additional references

(S1)   Perdew, J. P.; Ruzsinszky, A.; Csonka, G. I.; Vydrov, O. A.; Scuseria, G. E.; Constantin, L. A.; Zhou, X.; Burke, K. Restoring the density-gradient expansion for exchange in solids and surfaces. *Phys. Rev. Lett.* **2008**, *100*, No. 136406.

(S2)   Akola, J.; Jones, R., O.; Kohara, S.; Kimura, S.; Kobayashi, K.; Takata, M.; Matsunaga, T.; Kojima, R.; Yamada, N. Experimentally constrained density-functional calculations of the amorphous structure of the prototypical phase-change material $Ge_2Sb_2Te_5$, *Phys. Rev. B: Condens. Matter Mater. Phys.* **2009**, *80*, No. 020201.

(S3)   Akola, J.; Jóvári, P.; Kaban, I.; Voleská, I.; Kolář, J.; Wágner, T.; Jones, R. O. Structure, electronic, and vibrational properties of amorphous AsS_2 and $AgAsS_2$: Experimentally constrained density functional study. *Phys. Rev. B: Condens. Matter Mater. Phys.* **2014**, *89*, No. 064202.

(S4)   Matsunaga, T.; Akola, J.; Kohara, S.; Honma, T.; Kobayashi, K.; Ikenaga, E.; Jones, R. O.; Yamada, N.; Takata, M.; Kojima, R. From local structure to nanosecond recrystallization dynamics in AgInSbTe phase-change materials. *Nature Mater.* **2011**, *10*, 129-134.

(S5)   Gereben, O.; Jóvári, P.; Temleitner, L.; Pusztai, L. A new version of the RMC++ Reverse Monte Carlo programme, aimed at investigating the structure of covalent glasses, *J. Optoelectr. Adv. Mater.* **2007**, *9*, 3021-3027.

(S6)   Nosé, S. A molecular dynamics method for simulations in the canonical ensemble. *Mol. Phys.* **1984**, *52*, 255−268.

(S7)   Hoover, W. G. Canonical dynamics: equilibrium phase-space distributions. *Phys. Rev. A: Atom., Mol., Opt. Phys.* **1985**, *31*, 1695−1697.

(S8)   Yildirim, C.; Micoulaut, M.; Boolchand, P.; Kantor, I.; Mathon, O.; Gaspard, J.-P.; Irifune, T.; Raty, J.-Y. Universal amorphous-amorphous transition in $Ge_xSe_{100−x}$ glasses under pressure. *Sci. Rep.* **2016**, *6*, 27317.

(S9)   Yildirim, C.; Raty, J.-Y.; Micoulaut, M. Decoding entangled transitions: Polyamorphism and stressed rigidity. *J. Chem. Phys.* **2018**, *148*, No. 244505.
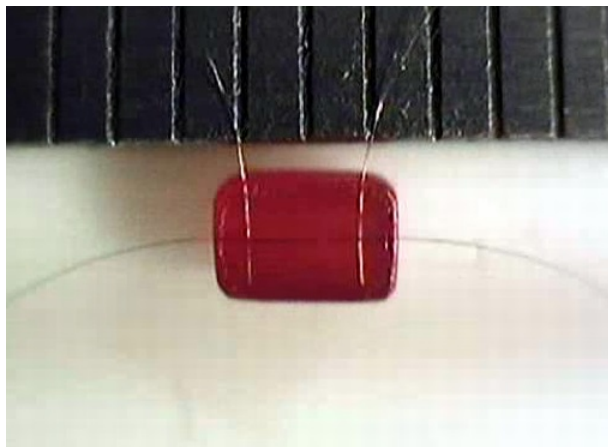
Figure S1. Glassy As_2S_3 sample for high-precision compressibility measurements.
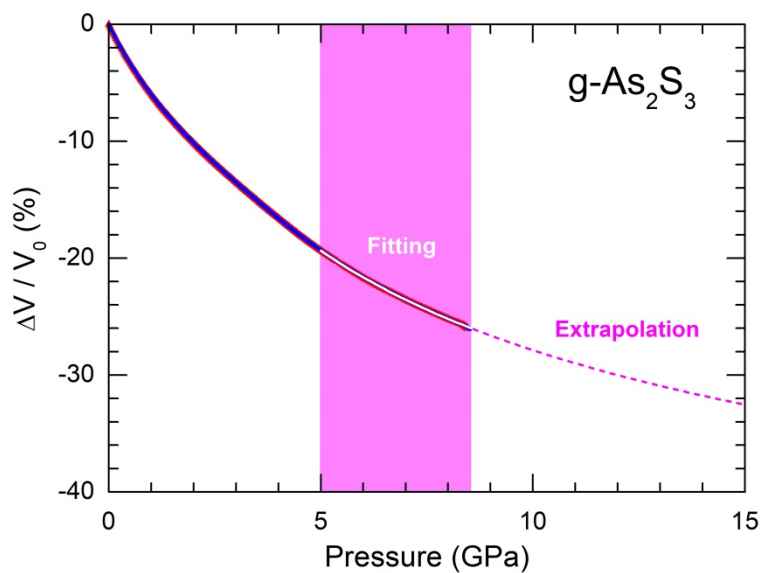

Figure S2. Compressibility extrapolation up to 15 GPa using a Murnaghan-type fitting with free V_0 of the experimental data points between 5.0 and 8.5 GPa, highlighted in magenta, and calculation of $\Delta V/V_0$ using the derived parameters. The experimental data points for two separate measurements without isobaric stops are shown by solid blue squares and red triangles, the fitting curve is white, the calculated compressibility function above 8.5 GPa is drawn by the dashed magenta line.
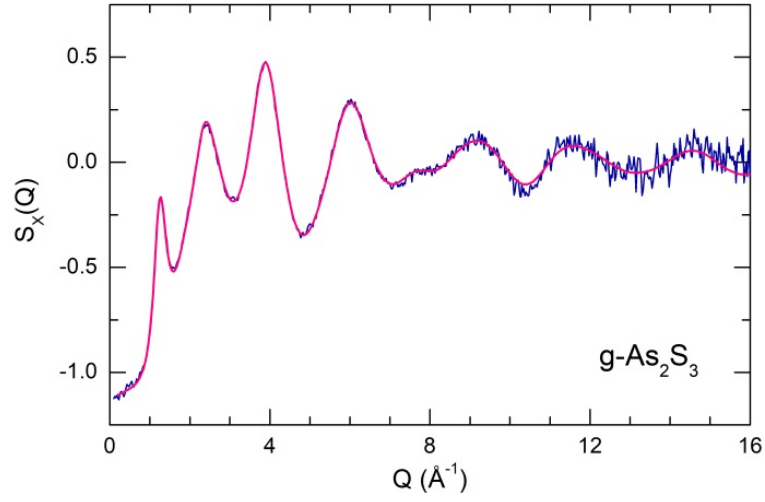
Figure S3. X-ray structure factors of glassy As_2S_3 at ambient pressure measured in a diamond anvil cell (blue) and using a conventional high-energy X-ray diffraction setup (pink).
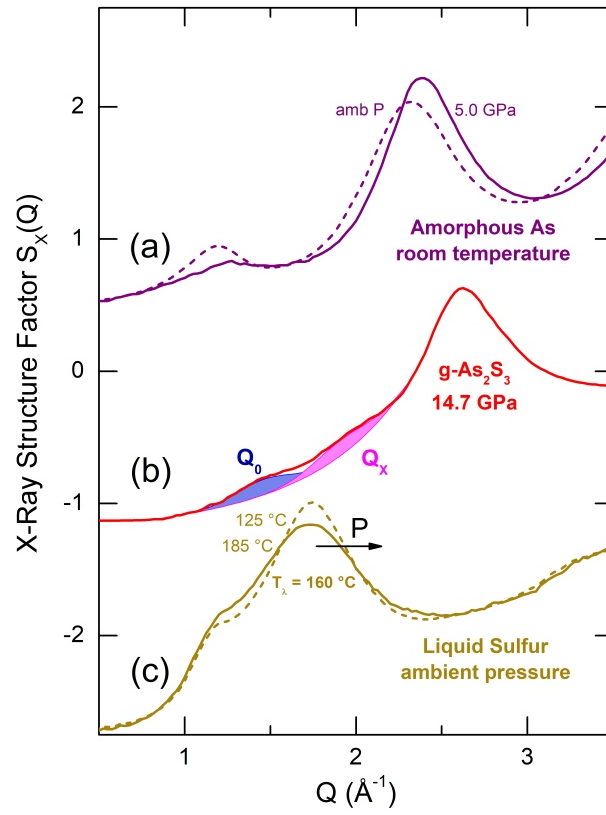

Figure S4. Comparison of the low-Q features in (a) amorphous arsenic at ambient pressure and 5.0 GPa, (b) glassy As_2S_3 at 14.7 GPa, and (c) liquid sulfur below (125 °C) and above (185 °C) the lambda-transition at 160 °C.
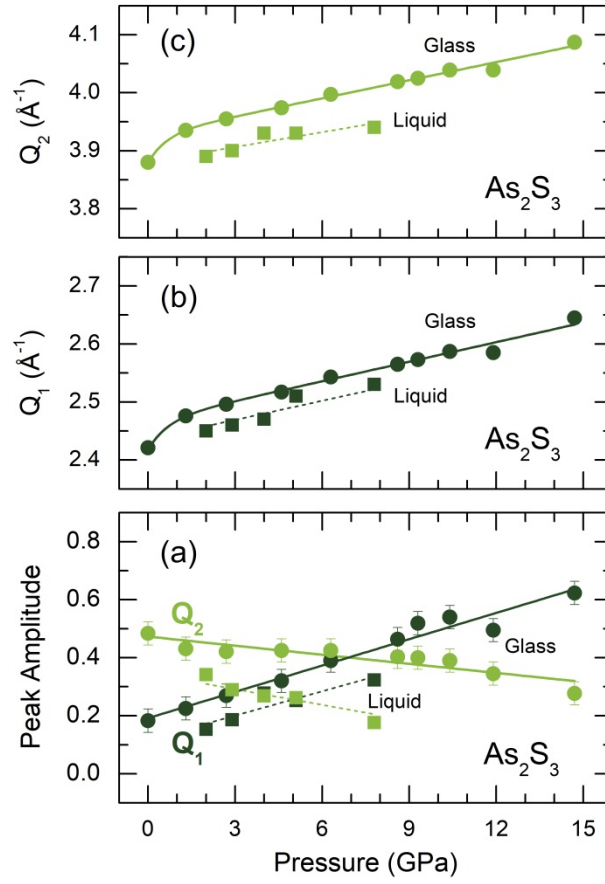
Figure S5. Pressure dependences of the principal peaks PP1 and PP2 in the structure factor of glassy (this work) and liquid[76] As_2S_3: (a) the peak amplitudes A_1 and A_2, (b) the PP1 position Q_1, and (c) the PP2 position Q_2. See text for further details.
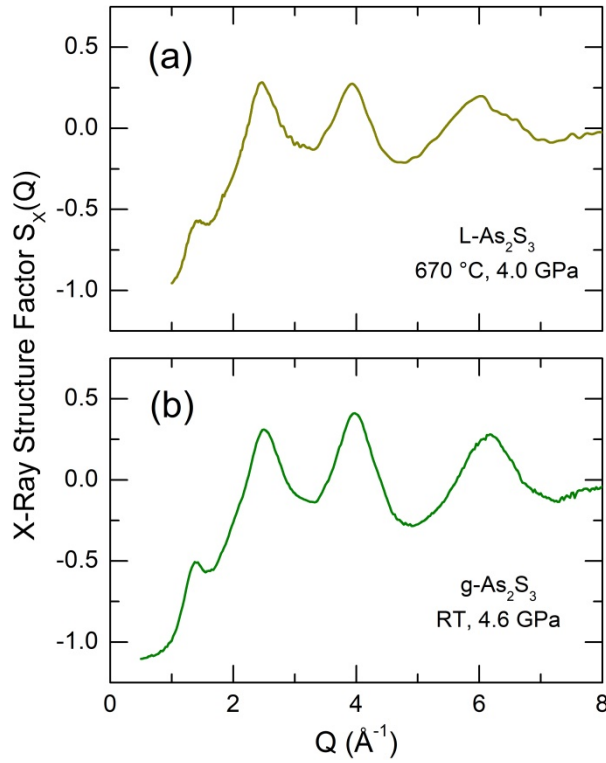

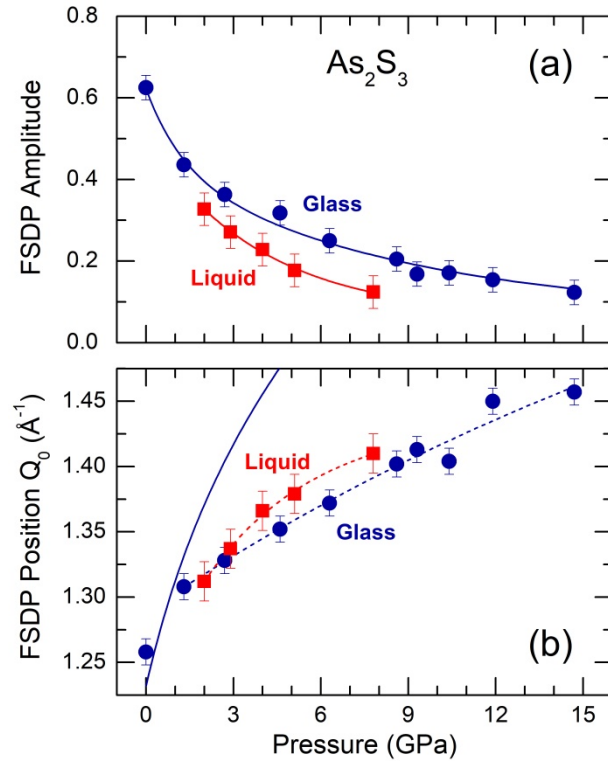**Figure S6**. X-ray structure factors of (a) liquid[76] and (b) glassy (this work) As_2S_3 at comparable pressure.

Figure S7. FSDP parameters for liquid[76] (red squares) and glassy (this work, blue circles) As₂S₃: (a) the A_0 amplitude, and (b) the Q_0 position as a function of pressure.
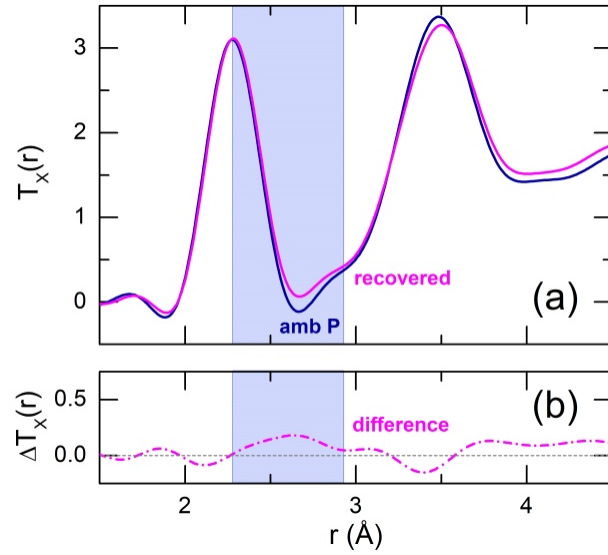

Figure S8. (a) Total correlation functions $T_X(r)$ for g-As₂S₃ at ambient pressure (blue) and recovered from 11.9 GPa (magenta) and (b) their difference, showing characteristic residual changes between the first and second neighbor peaks at 2.3 Å $\lesssim r \lesssim$ 2.9 Å, highlighted in blue and implying the enhanced chemical disorder on decompression.
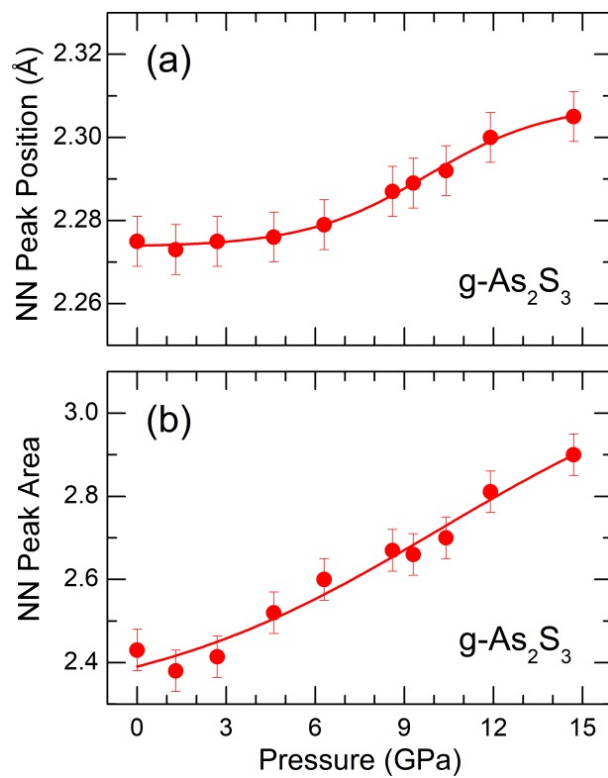
Figure S9. Apparent changes of the first neighbor peak at ≈2.28 Å with increasing pressure: (a) the peak position, (b) the integrated area of the peak until the first minimum at 2.63±0.01 Å. See text for further details.
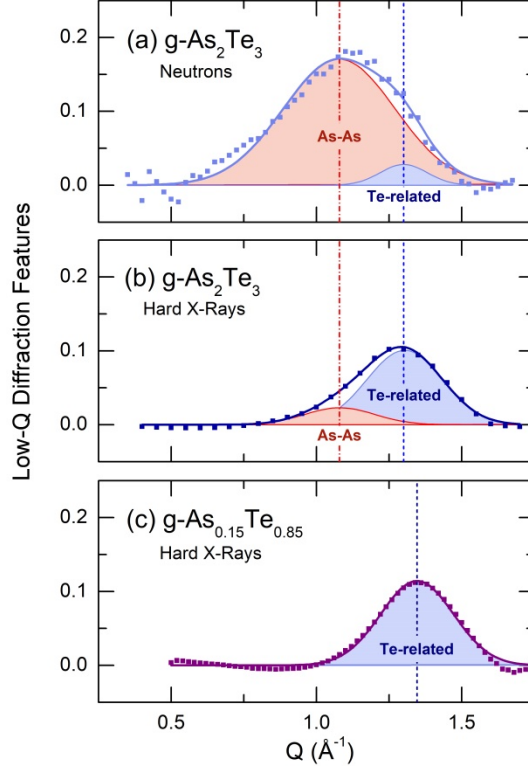
Figure S10. Low-Q diffraction features in glassy As_2Te_3:[32] (a) neutron data, (b) X-ray data, and (c) vitreous $As_{0.15}Te_{0.85}$ (X-ray data). The FSDP related to As-As periodicity is highlighted in red. The second low-Q feature highlighted in blue seems to be connected to Te-related correlations.

For glassy g-As_2Te_3, the FSDP shape and position are different in neutron $S_N(Q)$ and X-ray $S_X(Q)$ structure factors, Figure S10. Neutrons are more sensitive to arsenic ($\bar{b}_{As}/\bar{b}_{Te}$ = 1.134)[S10], while X-rays are better scattered by heavy tellurium (Z_{As}/Z_{Te} = 0.635), where $\bar{b}_i$ and Z_i are the coherent neutron scattering length and atomic number of element i, respectively. A significant chemical disorder in glassy arsenic telluride is reflected by bimodal asymmetric low-Q features: a usual FSDP at $Q_0 \approx 1.1$ Å⁻¹, related to As-As periodicity and clearly visible in $S_N(Q)$, and a second low-Q feature at $Q_x \approx 1.3$ Å⁻¹, more intense in the X-ray data and presumably related to Te-based correlations. In Te-rich glass, $As_{0.15}Te_{0.85}$, the As-As feature is no longer visible, and the remaining peak at 1.34 Å⁻¹ is symmetric. The difference structure factors $\Delta_{As}S(Q)$ and $\Delta_{Te}S(Q)$ derived around As and Te K-edges in g-As_2Te_3 using anomalous X-ray scattering[S11] are coherent with these findings. Consequently, the low-Q features are similar in glassy As_2Te_3 (ambient pressure) and As_2S_3 at 14.7 GPa. In other words, pressure-driven chemical disorder in vitreous arsenic sulfide is confirmed both in Q- and r-space.

Additional references

(S10)   Sears, V. F. Neutron Scattering Lengths and Cross Sections. *Neutron News* **1992**, *3*, 26−37.

(S11)   Ma, Q.; Raoux, D.; Bénazeth, S. Local Structure of As_xTe_{100-x} Glasses Studied by Differential X-ray Anomalous Scattering and X-ray Absorption Spectroscopy. *Phys. Rev. B: Condens. Matter Mater. Phys.* **1993**, *48*, 16332−16346.
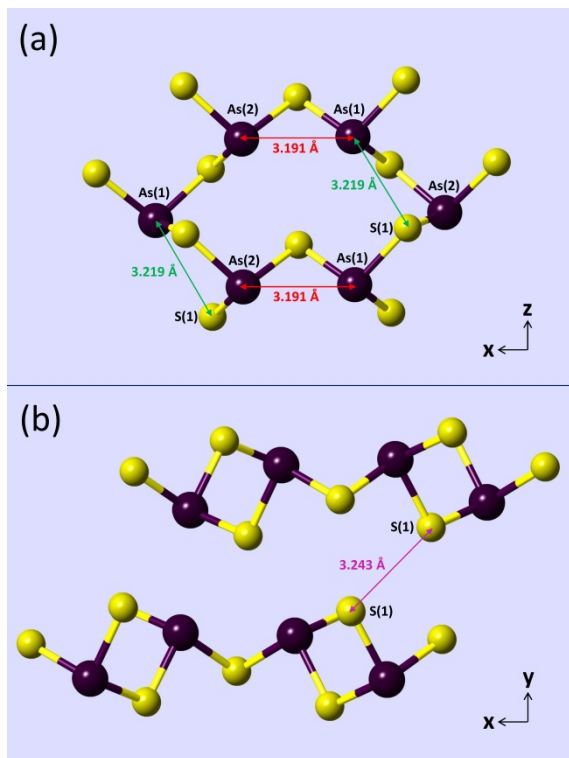
Figure S11. Crystal structure of monoclinic orpiment As_2S_3:[108] (a) a single 12-membered ring As_6S_6 within a 2D layer parallel to the (x,z)-plane; (b) two consecutive layers perpendicular to the (x,y)-plane. The shortest As-As and As-S second neighbor separations and S-S interlayer contacts are shown.
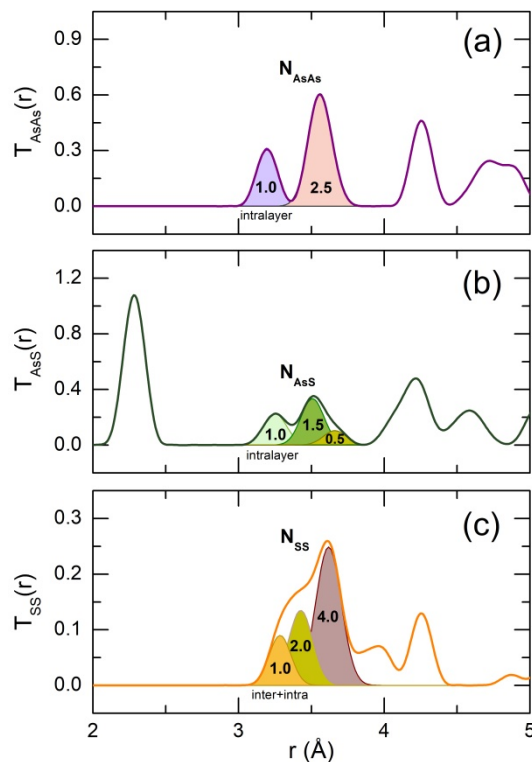
Figure S12. Neutron-weighted partial correlation functions $T_{ij}(r)$ in monoclinic As_2S_3:[108] (a) As-As, (b) As-S, and (c) S-S, calculated using the XTAL code.[S12] The coordination numbers of the second neighbors and short interlayer contacts are indicated within the corresponding r-space features.

Additional references

(S12)   Hannon, A. C. XTAL: a Program for Calculating Interatomic Distances and Coordination Numbers for Model Structures. *Rutherford-Appleton Laboratory Report RAL-93-063*, 1993.